



HAL
open science

Confinement of *Candida Antarctica* Lipase B in a Multifunctional Cyclodextrin-Derived Silicified Hydrogel and Its Application as Enzymatic Nanoreactor

Cédric Decarpigny, Rudina Bleta, Anne Ponchel, Eric Monflier

► To cite this version:

Cédric Decarpigny, Rudina Bleta, Anne Ponchel, Eric Monflier. Confinement of *Candida Antarctica* Lipase B in a Multifunctional Cyclodextrin-Derived Silicified Hydrogel and Its Application as Enzymatic Nanoreactor. *ACS Applied Bio Materials*, 2019, 2 (12), pp.5568-5581. 10.1021/ac-sabm.9b00646 . hal-02421245

HAL Id: hal-02421245

<https://hal.science/hal-02421245>

Submitted on 13 Nov 2023

HAL is a multi-disciplinary open access archive for the deposit and dissemination of scientific research documents, whether they are published or not. The documents may come from teaching and research institutions in France or abroad, or from public or private research centers.

L'archive ouverte pluridisciplinaire **HAL**, est destinée au dépôt et à la diffusion de documents scientifiques de niveau recherche, publiés ou non, émanant des établissements d'enseignement et de recherche français ou étrangers, des laboratoires publics ou privés.

Confinement of *Candida Antarctica* Lipase B in a Multifunctional Cyclodextrin-Derived Silicified Hydrogel and its Application as Enzymatic Nanoreactor

Cédric Decarpigny,[†] Rudina Bleta,^{*†} Anne Ponchel[†] and Eric Monflier[†]

[†]Univ. Artois, CNRS, Centrale Lille, ENSCL, Univ. Lille, UMR 8181-UCCS-Unité de Catalyse et Chimie du Solide, F-62300 Lens, France.

KEYWORDS: supramolecular hydrogel, cyclodextrin, silica, enzyme, confinement, nanoreactor, biocatalysis, 2-diformylfuran, 2,5-furandicarboxylic acid.

ABSTRACT

Supramolecular hydrogels with a three-dimensional cross-linked macromolecular network have attracted growing scientific interest in recent years due to their ability to incorporate high loadings of bioactive molecules such as drugs, proteins, antibodies, peptides and genes. Herein, we report a versatile approach for the confinement of *Candida antarctica* lipase B (CALB) within a silica-strengthened cyclodextrin-derived supramolecular hydrogel and demonstrate its potential

application in the selective oxidation of 2,5-diformylfuran (DFF) to 2,5-furandicarboxylic acid (FDCA) under mild conditions. The enzymatic nanoreactor was deeply characterized using thermogravimetric analysis, Fourier transform infrared spectroscopy, N₂-adsorption, dynamic light scattering, UV-visible spectroscopy, transmission electron microscopy, scanning electron microscopy and confocal laser scanning microscopy, while the reaction products were established on the basis of ¹H nuclear magnetic resonance spectroscopy combined with high-performance liquid chromatography. Our results revealed that whilst CALB immobilized in conventional sol-gel silica yielded exclusively 5-formylfuran-2-carboxylic acid (FFCA), confinement of the enzyme in the silicified hydrogel imparted a five-fold increase in DFF conversion and afforded 67% FDCA yield in 7 hours and almost quantitative yields in less than 24 hours. The hierarchically interconnected pore structure of the host matrix was found to provide a readily accessible diffusion path for reactants and products, while its flexible hydrophilic-hydrophobic interface was extremely beneficial for the interfacial activation of the immobilized lipase.

Introduction

Enzymes are highly efficient and selective biocatalysts capable of operating under mild reaction conditions, *i.e.* ambient temperature, atmospheric pressure and physiological pH.^{1,2} Their excellent regio- and stereo-selectivity, together with high substrate specificity and low environmental toxicity, make them suitable for a broad range of chemical reactions.^{1,3,4} However, the short catalytic lifetime of enzymes, their low stability towards high temperatures, organic solvents and extreme pHs and the difficulties related to their recovery and reuse are limiting factors for their industrial applications.^{1,3,5} Immobilization in a support provides an effective way to increase the stability of the enzyme under harsh industrial conditions and facilitate its recovery and reuse.⁶

In living cells, enzymes are confined in highly organized functional compartments (cellular or subcellular) where metabolic processes are very tightly regulated.⁷ Intracellular compartmentalization of cooperative enzymes within the cell enables control of the speed with which biochemical reactions occur and the order in which specific enzymes will react. Structural studies have revealed the critical role played by the pores in regulating the transfer of metabolites inside and outside those compartments.⁸

Inspired by the enzymatic systems encountered in nature, several authors have proposed biomimetic approaches based on encapsulation of the biocatalyst in soft-matter assemblies or immobilization in a pre-synthesized inorganic support.⁹⁻¹¹ However, in the industrial context, immobilization in a pre-existing carrier remains the most widely employed technique for enzyme immobilization. Most common examples of supports are synthetic resins, biopolymers such as polysaccharides and inorganic solids such as mesoporous silicas or zeolites.⁶ In addition to their beneficial effect on enzyme confinement, pores may also have a relevant importance in the stability of the biocatalyst,¹² as well as the diffusion of reactants and products during the catalytic process.^{13,14} Nevertheless, it should be noted that immobilization in solid matrices does not always guarantee intact function of the enzyme due to multiple conformational changes caused by the surface roughness of the support.^{9,10}

Taking into account the sensitivity of proteins to rigid surfaces, organic-inorganic hybrid materials have been extensively used as promising carriers for enzyme immobilization as they combine the softness of the organic phase and the mechanical strength of the mineral one.^{9,15-18} For example, Luckarift *et al.*⁹ showed that butyrylcholinesterase immobilized in biomimetic silica prepared by silicification of silaffin polypeptides could retain almost 90% of its initial activity compared to only 10% activity for the enzyme immobilized on conventional sol-gel silica.

Similarly, Kim *et al.*,¹⁵ developed a novel strategy for covering individual enzymes with a thin layer of a porous organic-inorganic network. The resulting hybrid nanostructure presented minimal substrate mass transfer limitations and exhibited extremely high stability compared to the free enzyme in aqueous buffer. In another study, Ackerman *et al.*¹⁶ highlighted synergistic effects between functionalized mesoporous silica and urea toward favorable conformational changes in glucose isomerase, which resulted in a remarkable increase of the enzyme activity in confined space. Bradshaw *et al.*¹⁷ elaborated hierarchically porous MOF-based capsules around a Pickering-stabilized hydrogel inside which *Candida antarctica* lipase B was encapsulated and demonstrated the practical utility of this biocatalyst in size-selective transesterification reactions. Recently, Du *et al.*¹⁸ proposed a new approach toward the immobilization of lipases in a hollow MOF-based composite using metal-sodium deoxycholate (NaDC) hydrogel as soft template. Interestingly, the hydrogel was found to offer a comfortable microenvironment to the lipase during the MOF growth and a better protection against the external environment.

Supramolecular hydrogels are three-dimensional hydrophilic polymer networks capable of retaining large amounts of water.¹⁹ Due to their multifunctional properties, those cross-linked systems have undergone a spectacular progress in recent years showing high potential as scaffolds for tissue engineering,²⁰ biomaterials for medical devices and drug delivery systems,²¹ supramolecular templates for biomineralization,²² assay for detection of enzyme inhibitors²³ and skeleton of artificial enzymes.²⁴ More specifically, for catalytic applications, supramolecular hydrogels have demonstrated a “superactivity” when used as host matrices for the immobilization of biocatalysts.²⁵

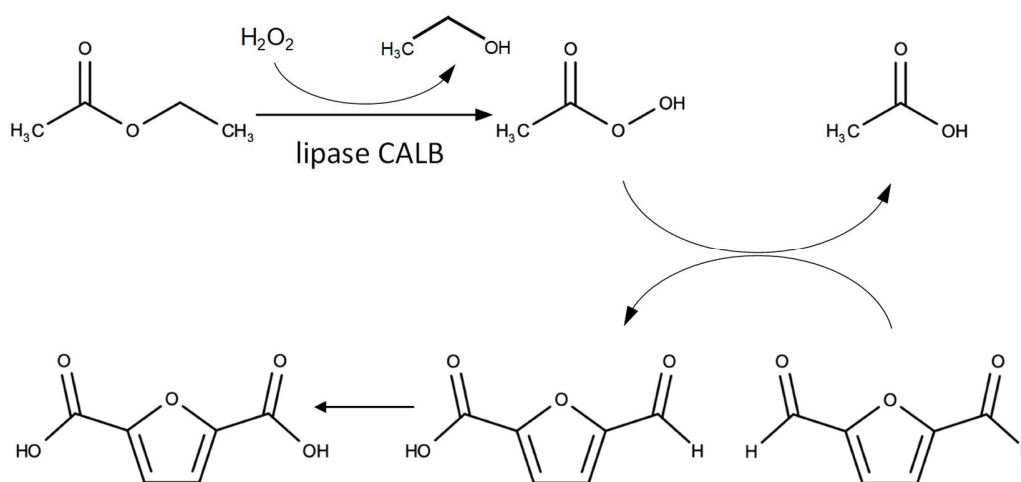
In recent years, self-assembled supramolecular hydrogels based on polymer-cyclodextrin inclusion complexes have emerged as promising systems for drug delivery applications.²⁶

Cyclodextrins (CDs) are water-soluble cyclic oligosaccharides composed of n glucopyranose units exhibiting a hydrophobic internal cavity and a hydrophilic exterior surface. The most common cyclodextrins are alpha-, beta- and gamma-CD possessing respectively 6, 7 and 8 glucose units in their ring. In addition to their ability to form a multitude of supramolecular assemblies with a wide range of polymers,²⁷ CDs have been utilized as versatile tools for engineering artificial enzymes due to their hydrophobic cavity which mimics the hydrophobic pocket of the enzyme.²⁸ Moreover, native CDs can also form *polypseudorotaxanes* with necklace-like structures with amphiphilic block copolymers such as Poloxamers. It is well-known that α -CD preferentially binds the hydrophilic ethylene oxide (EO) blocks of the polymer, while β -CD, due to its larger cavity, slides along the EO units to selectively thread the middle hydrophobic propylene oxide (PO) blocks.²⁸ Under optimal conditions, the aggregation of *polypseudorotaxanes* induces the spontaneous formation of a three-dimensional hydrogel network where water-insoluble nanocrystallites act as physical cross-linkers maintaining the hydrogel in a water-swollen state.²⁹⁻³¹

Herein, we describe the preparation and characterization of a silicified pluronic F127/ α -CD hydrogel composed of a dual organic-inorganic cross-linked network and demonstrate its use as a carrier for the confinement of the lipase B from *Candida antarctica* (CALB). Unlike the encapsulation approach, which implies entrapment of the enzyme within the silica framework during the sol-gel synthesis, the strategy described herein relies on immobilization in a prefabricated carrier⁶ since the lipase is immobilized upon the hydrogel is silicified and functionalized.

Lipases (triacylglycerol acylhydrolases EC 3.1.1.3) belong to the family of hydrolases whose natural function is to catalyze the hydrolysis of carboxylic ester bonds. They are probably the most important industrial enzymes in food, detergent and pharmaceutical sectors owing to their

specificity not only in hydrolysis, but also in esterification, transesterification and interesterification reactions.^{32,33} CALB is a member of the lipase family that has been used in a broad range of biotransformations of industrial importance due to its high selectivity toward secondary alcohols and secondary amines, as well as lack of sensitive cofactor requirements.^{34,35} In this study, we evaluated its activity in the selective oxidation of the 2,5-diformylfuran (DFF) to the 2,5-furandicarboxylic acid (FDCA), a promising alternative to the fossil-based terephthalic acid (TPA) in the production of poly(ethylene terephthalate) (PET) plastics.³⁶ Actually, this transformation is a chemo-enzymatic cascade reaction (*Scheme 1*).³⁷ First, the lipase CALB catalyzes the conversion of ester (ethyl acetate) to peracid (peracetic acid) using hydrogen peroxide as oxygen donor. Then, the peracid generated *in-situ* is responsible for the oxidation of the aldehyde group of DFF to carboxylic acid yielding 5-formylfuran-2-carboxylic acid (FFCA), which is ultimately converted to FDCA.³⁸ Commercially available immobilized CALB (Novozym 435) has been successfully employed in the oxidation of DFF with excellent selectivity for FDCA.³⁹



Scheme 1. Chemo-enzymatic oxidation of DFF. First, the lipase CALB catalyzes the peracid formation, then the peracid is responsible for the oxidation of DFF to FDCA.

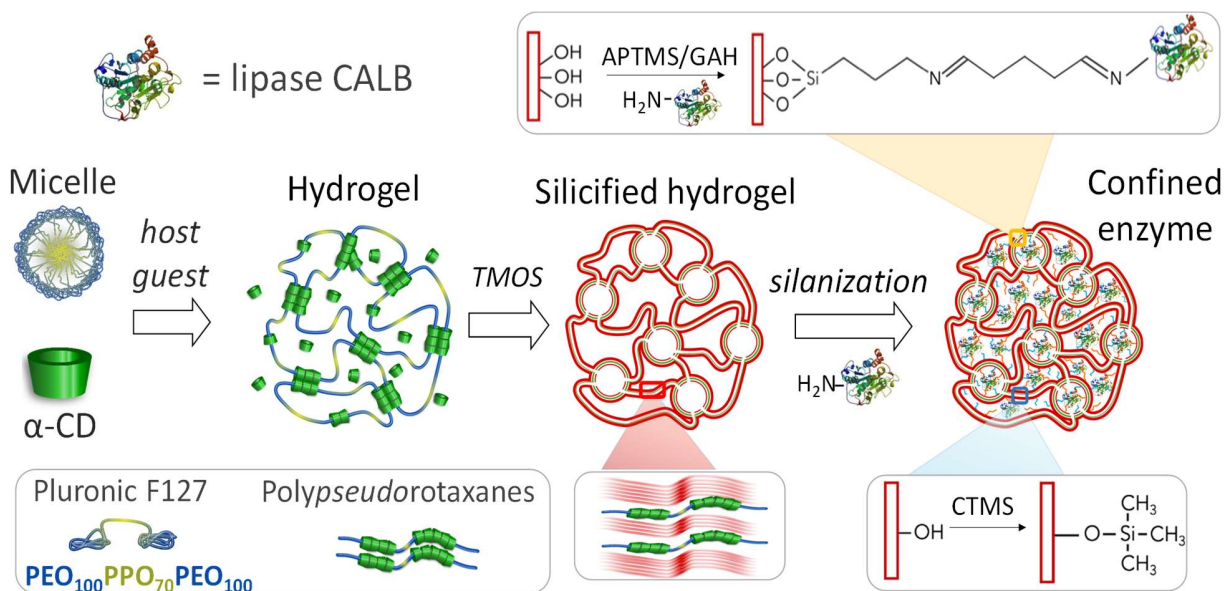
To our knowledge, this is the first study describing the possibility of using a silicified CD-based supramolecular hydrogel as a carrier for the confinement of a lipase and its application in the selective oxidation of DFF to FDCA. Our results suggest that these supramolecular systems may be considered as interesting candidates for the immobilization of other lipases to catalyze reactions in confined environments.

Results and discussion

Method for the confinement of CALB in the silicified hydrogel

The overall synthesis pathway for the covalent confinement of lipase CALB in the silicified hydrogel is schematically illustrated in Scheme 2 (see ESI for experimental details). First, a three-dimensional physically cross-linked hydrogel was prepared in a saturated α -CD aqueous solution (100 mg/mL) by host-guest inclusion-induced self-assembly between the block copolymer pluronic F127 and the native α -CD. Subsequently, tetramethylorthosilicate (TMOS) was added as the silica source to form a silica shell within the layered structure of polypseudorotaxanes. After removal of the excess of polymer and α -CD, a porous hybrid silica-hydrogel material was recovered where the CD-based polypseudorotaxanes were incorporated within the silica framework, while the non-threaded α -CD could be distributed both inside and outside the pores. The hybrid material was then modified with two different functions,⁴⁰ (i) chemically reactive amine groups activated with glutaraldehyde necessary for the covalent anchoring of the lipase CALB and (ii) hydrophobic trimethyl groups necessary for its interfacial activation. The activity of the grafted biocatalyst was then evaluated in the oxidation of 2,5-diformylfuran (DFF) to 2,5-furandicarboxylic acid (FDCA) and compared to that of the enzyme immobilized by ionic binding.

In this approach, the function of the hydrogel was not only to act as a template for the formation of a porous network into which the protein can be confined, but also to boost the activity of the lipase through creation of a flexible environment with appropriate hydrophilic/hydrophobic balance necessary for its interfacial activation. Moreover, the hierarchical structure with open interconnected porosity should also permit higher enzyme loadings and ensure optimal diffusion of reactants and products during the catalytic process due to acceleration of mass transfer between the inside and the outside of the pores.



Scheme 2. Schematic illustration of the preparation procedure for the confinement of lipase CALB into the silicified hydrogel silanized with hydrophobic and chemically reactive groups. For the sake of clarity, only the silica wall is shown in the two insets depicting the surface functionalization.

Preparation and characterization of the silicified hydrogel

To study the change of pluronic F127 micellar structure upon addition of α -CD, Dynamic Light Scattering (DLS) measurements were performed at 25 °C. We chose a starting concentration of 1.6 wt.% in polymer which was above its critical micellar concentration (CMC) reported in literature (0.7 wt.% at 25 °C).⁴¹ Contrary to the randomly methylated β -CD (RaMe β -CD), which was previously shown to locate at the interface layer of pluronic P123 micelles,⁴² the native α -CD tends to selectively thread the hydrophilic EO blocks and form *polypseudorotaxanes* with a well-ordered channel structure.²⁷

Figure 1 displays the intensity size distribution plots of the micellar solutions prepared with 1.6 wt.% pluronic F127 and increasing concentrations of α -CD, from 5 mg/mL (α -CD/EO molar ratio = 0.02) to 40 mg/mL (α -CD/EO = 0.16). Prior to α -CD addition, the F127 solution displayed two main peaks with apparent hydrodynamic radius (R_H) of 3.5 nm and 22 nm (Figure 1 A, a) that can be ascribed to unimers and micelles respectively. When a small amount of α -CD (5 mg/mL, α -CD/EO = 0.02) was added to this solution, the size of the micelles was not much modified, but the scattering intensity slightly decreased indicating the beginning of the complexation process (Figure 1 A, b). In parallel, new supramolecular structures were formed ($R_H = 205$ nm) resulting from the stretching of the EO blocks from the micellar corona after complexation with α -CD and further agglomeration. Further increase of α -CD concentration from 10 to 20 mg/mL (α -CD/EO = 0.04 to 0.08) resulted in a reduction of the scattering of the micelles caused by the loss of their spherical shape. On the other hand, the scattering of the new species formed showed a marked increase and was very broad indicating the formation of structures with a wide range of sizes (Figure 1 A, c-e). Over longer time scales (4 hours and 24 hours), further structural rearrangements occurred which again indicated polydispersity in size (Figure S1, ESI). In the concentration range between 25

mg/mL (α -CD/EO = 0.10) and 40 mg/mL (α -CD/EO = 0.16) (Figure 1 B, a-d), the fraction of remaining micelles was negligible and R_H shifted to larger sizes (260-295 nm) indicating total dissociation of the micelles. Mixtures progressively became turbid with aging due to the formation, growth and aggregation of insoluble *polypseudorotaxanes* (Figure S2, ESI). Beyond 40 mg/mL α -CD, all mixtures were turbid and turned to hydrogel after different duration times. Kinetically, the sol-gel transition was favored by low temperatures and high α -CD to EO molar ratios.²⁶ Thus, the sample prepared with 50 mg/mL α -CD (α -CD/EO = 0.20) was still fluid after 72 hours, while samples prepared with 60 mg/mL α -CD (α -CD/EO = 0.24) and above completely transformed to hydrogel (Figure S3, ESI). For the highest α -CD concentration studied (100 mg/mL, α -CD/EO = 0.40), *polypseudorotaxanes* formed very rapidly, in a high yield, and only after 16 hours, the mixture displayed an elastic solid-like behavior due to the formation of a three-dimensional hydrogel network (Figure 1 C). It is worth underlying that compared to PEG/ α -CD hydrogels that require high polymer concentrations,⁴³ pluronic F127/ α -CD hydrogel can be formed with a polymer concentration as low as 1.6 wt.% due to the occurrence of hydrophobic interactions between unthreaded PO units in addition to hydrogen bond interactions between threaded α -CD which facilitates the formation of the hydrogel network.⁴³ Given the high compactness of the hydrogel prepared with 100 mg/mL α -CD and 1.6 wt.% pluronic F127 after a relatively short time (16 hours), we opted for this formulation to pursue our study.

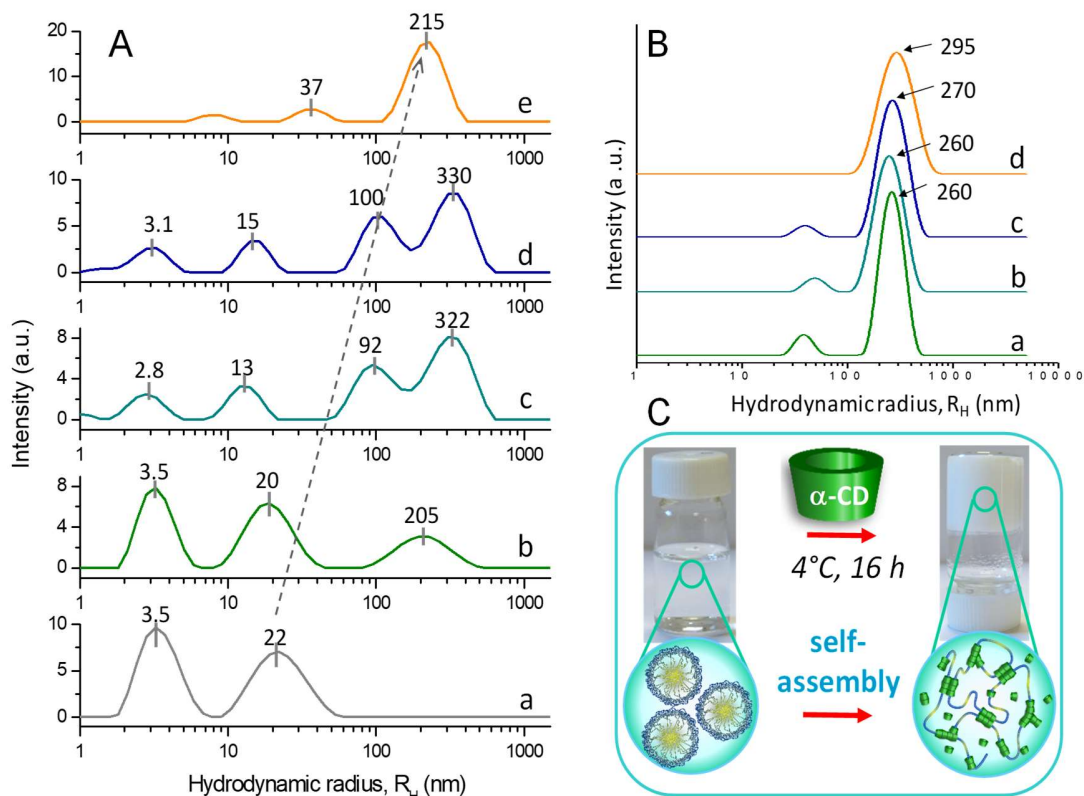


Figure 1. Apparent hydrodynamic radius distributions of the scattered intensity at 25 °C for the supramolecular assemblies prepared with 1.6 wt.% pluronic F127 and increasing concentrations of α -CD: (A) from 0 to 20 mg/mL α -CD: (a) 0 mg/mL; (b) 5 mg/mL; (c) 10 mg/mL; (d) 15 mg/mL; (e) 20 mg/mL; (B) from 25 to 40 mg/mL α -CD: (a) 25 mg/mL; (b) 30 mg/mL; (c) 35 mg/mL; (d) 40 mg/mL; (C) Visual aspect of the block copolymer solution (1.6 wt.%) before and after addition of α -CD (100 mg/mL).

The supramolecular hydrogel was then silicified using TMOS as silica source.⁴⁴ After collection of the precipitate and removal of the excess of hydrogel by rinsing with deionized water, the hybrid material was recovered in the form of a powder. The FTIR spectra of the materials prepared with and without hydrogel are shown in Figure 2. For both materials, the intense bands observed at 1056 cm^{-1} and 798 cm^{-1} can be ascribed to the asymmetric and symmetric stretching vibrations

respectively of the Si-O-Si bond, while the band at 953 cm^{-1} arises from the symmetric stretching of the Si-OH groups.⁴⁵ The increase in intensity of the band at 1056 cm^{-1} in the silicified hydrogel (Figure 2 A a) may be explained by the overlapping of the asymmetric Si-O-Si stretching vibration of silica with the ring vibrational modes in the composition of cyclic structures (glycosyl units in α -cyclodextrin).⁴⁶ On the other hand, the O-H stretching vibration of physisorbed water and surface silanols in interaction with water (SiO-H...H₂O) appeared in the region $3600\text{-}3200\text{ cm}^{-1}$. Other bands in the region $2974\text{-}2893\text{ cm}^{-1}$, which were not observed in the hydrogel-free SiO₂, are typical of the C-H vibration from both α -CD and pluronic F127.

From the TG analysis (Figure 2 B), the amount of the incorporated hydrogel was estimated by the difference between the mass loss of the silicified hydrogel minus the mass loss of the sol-gel silica prepared without hydrogel. In the temperature range between 180 and $700\text{ }^{\circ}\text{C}$, the hybrid material displayed a weight loss of $17.8\text{ wt.}\%$ which can be attributed to the thermal removal of the template and OH groups, while the pristine sol-gel SiO₂ revealed a weight loss of $4.2\text{ wt.}\%$ corresponding mainly to the removal of OH groups. Thus, the mass percentage of hydrogel remaining in the hybrid material was calculated to be $13.6\text{ wt.}\%$.

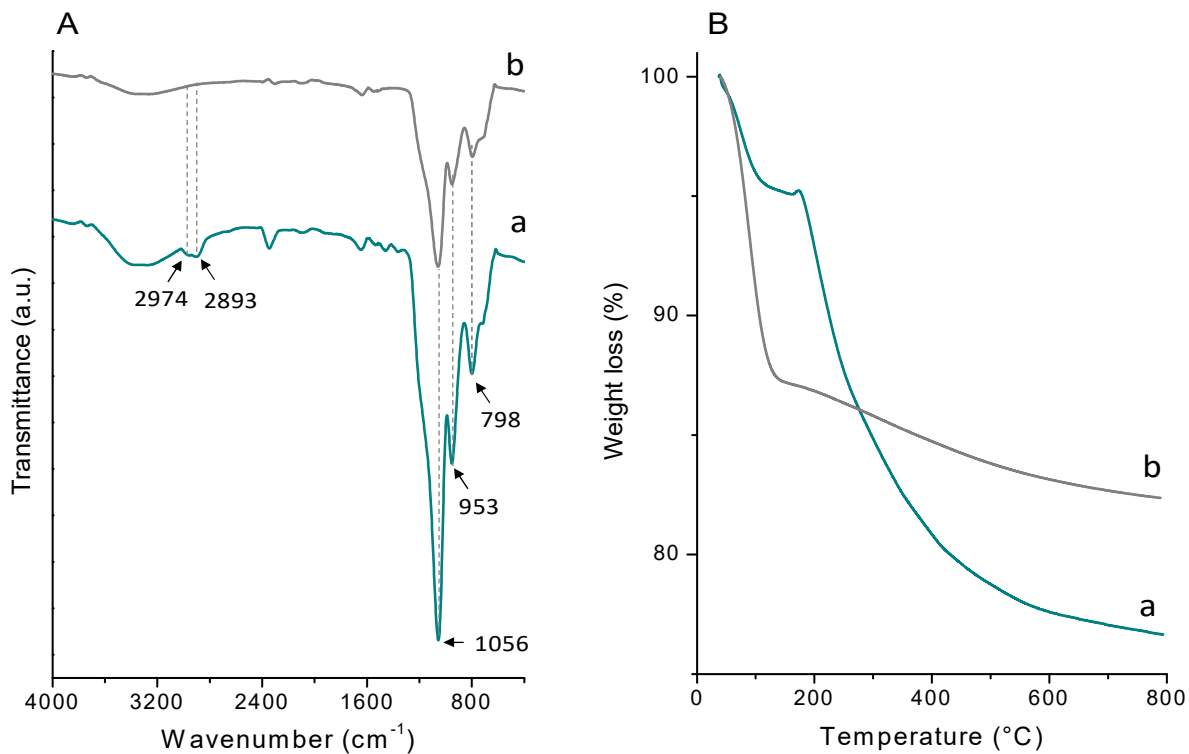


Figure 2. ATR-FTIR spectra (A) and TGA curves (B) of the silicified F127/ α -CD hydrogel (a) and hydrogel-free sol-gel silica (b).

N₂-adsorption analyses were then carried out to determine the textural characteristics of the silicified hydrogel. Differently from materials prepared from pluronic F127 and α -CD separately, which showed monomodal size distributions (56 nm diameter for pluronic F127 and 3.4 nm for α -CD) (Figure S4, ESI), the silicified hydrogel presented two types of mesopores with 3.8 nm and 20-60 nm diameter derived from individual *polypseudorotaxanes* and channel-like nanocrystallites respectively (Figure 3).⁴⁴ Note that this second pore size distribution was very broad due to the heterogeneity in size of nanocrystallites having different crosslinking densities. In addition to mesopores, micropores with diameters less than 2 nm were also present and could result from the insertion of non-complexed α -CD and EO groups into the walls of silica.⁴⁷ Macropores also exist,

as revealed by the continuous increase of the adsorbed volume at high relative pressures ($P/P_0 \approx 1$). The BET surface area (S_{BET}) and total pore volume (V_p) for this material were $136 \text{ m}^2/\text{g}$ and $0.156 \text{ cm}^3/\text{g}$ respectively, while the micropore volume determined by the *t*-plot method was about 7.1 % of the total pore volume (Table S1, ESI). Compared with the mesoporous silica prepared from α -CD alone, which presented a surface area of $287 \text{ m}^2/\text{g}$ and a type IV isotherm, the surface area of the silicified hydrogel was much lower, but the cross-linking of polypseudorotaxanes into a three-dimensional network generated a unique structure with high pore interconnectivity. On the other hand, the control sol-gel silica prepared without hydrogel presented a higher surface area ($634 \text{ m}^2/\text{g}$) with respect to the silicified hydrogel, but this material was mainly composed of micropores (14.8%) which do not match with the large dimensions of the enzyme (Table S1, ESI). Finally, the silicified hydrogel calcined at $500 \text{ }^\circ\text{C}$ also showed a multimodal pore structure (Figure S4, ESI) with a very high surface area and pore volume ($1083 \text{ m}^2/\text{g}$ and $1.09 \text{ cm}^3/\text{g}$ respectively) due to the large amount of micropores (15.6 %) and small mesopores (3.8 nm) resulting from the shrinkage during calcination.

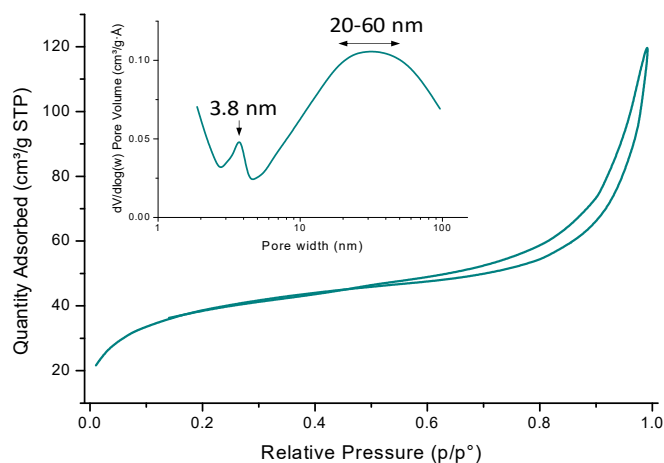


Figure 3. N₂-adsorption isotherm and corresponding pore size distribution (inset) of the silicified F127/ α -CD hydrogel.

Interestingly, FE-SEM images of the silicified hydrogel revealed uniformity in the intergrowth of silica particles into features with a flowerlike morphology (Figure 4). The average size of particles ranged from 30 to 50 μm (Figure 4 a). Nanoflowers were composed of rose petals with 2-3 μm length and 40-50 nm thickness (Figure 4 b) originating from the layered structure of *polypseudorotaxanes* within the supramolecular hydrogel. In the most ordered regions, macropores resulting from the packing of primary particles (voids originally occupied by water in the hydrogel) presented an average diameter of 1-3 μm (Figure S5, ESI). At higher magnification, TEM images (Figure 4 c-h) revealed that the silicified hydrogel was able to spread out and adapt a fibrous-like structure due to the dissociation of the micelles and the formation of *polypseudorotaxanes*. Further association of the *polypseudorotaxanes* into bundles led to long and thick tubular silica structures with 10-50 nm diameter (Figure 4 c). Compared with structures obtained previously from PEG/ α -CD hydrogels at pH 2.0 and 4.0,⁴⁴ the silica fibers formed here (pH 7) were much thicker, suggesting a higher level of α -CD threading and aggregation. Interestingly, it is important to remark that, although the hydrogel was silicified, it still maintained a high level of flexibility, as evidenced by the folded and curved patterns formed throughout its structure (Figure 4, d-f). The interconnection of individual fibers generated large mesopores (white spots) with a heterogeneous pore geometry and 10-50 nm diameter (Figure 4 g), together with small mesopores with a random structure and less than 5 nm diameter (Figure 4 h) in agreement with N_2 adsorption analysis. These observations clearly indicate that the silica material could readily adapt the morphology of the native supramolecular hydrogel under the conditions employed in our synthesis.

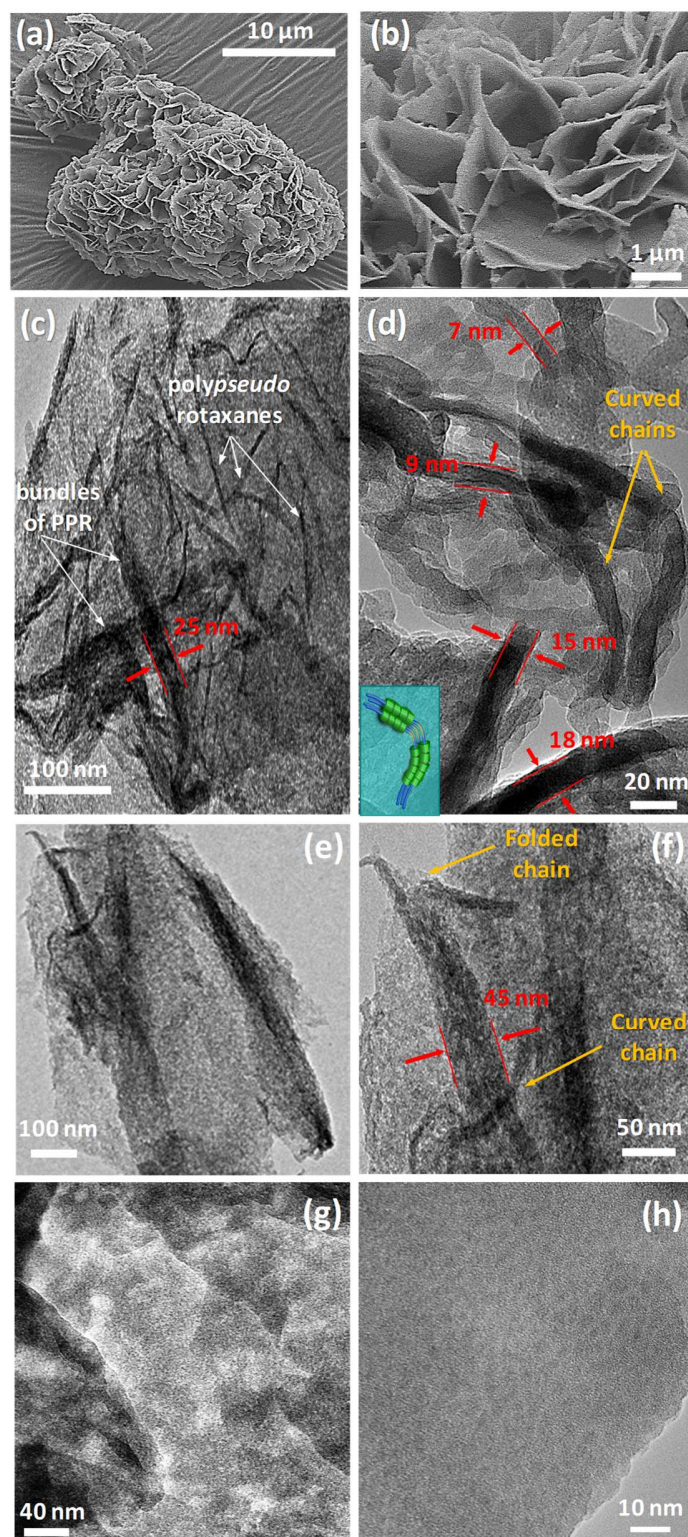


Figure 4. FE-SEM (a, b) and TEM images (c-h) of the silicified F127/ α -CD hydrogel.

Silanization of the support and enzyme immobilization

Next, the silicified hydrogel was silanized with hydrophobic (chlorotrimethylsilane, CTMS) and chemically reactive groups (3-aminopropyltrimethoxysilane, APTMS) using glutaraldehyde (GAH) as a linker. Silanization implies the formation of a layer of organosilane through a condensation reaction. To identify the different functional groups incorporated in the silicified hydrogel, we performed attenuated total reflectance Fourier transform infrared spectroscopy (ATR-FTIR) and thermogravimetric (TG) analysis (Figure 5).

Trimethylsilyl groups on the CTMS-modified material (Sihgel@C) were confirmed by the presence of symmetric and asymmetric C-H stretching vibrations from aliphatic -CH₃ groups at 2880 cm⁻¹ and 2955 cm⁻¹ respectively, as well as the Si-C stretching vibration at 850 cm⁻¹ from -O-SiCH₃ end groups (Figure 5 A,a).⁴⁵ Note that the surface silanols at 3400 cm⁻¹ and 953 cm⁻¹ were reduced compared to non-modified silica (Figure 2) indicating decrease in surface hydrophilicity. On the other hand, the material functionalized with APTMS and activated with GAH (Sihgel@AG) displayed a relatively strong band at 1553 cm⁻¹ consistent with the N-H bending of the primary amine (Figure 5 A,b) which was also observed on Sihgel@A prepared without GAH (Figure S6, ESI). In addition, the band observed at 1406 cm⁻¹ is typical of the symmetric CH₂ bending of Si-CH₂ groups.⁴⁵ The covalent anchoring of glutaraldehyde was confirmed by the band at 1644 cm⁻¹ assigned to the imine bond (C=N) resulting from the interaction between the primary amine groups of Sihgel@A and the aldehyde groups of GAH. Moreover, the Sihgel@CAG material displayed the typical vibration bands of N-H (1553 cm⁻¹), CH₂ (1406 cm⁻¹) and Si-C (850 cm⁻¹) indicating that both grafting and hydrophobic functions were successfully anchored on the host matrix (Figure 5 A,c). Upon enzyme immobilization

(Sihgel@CAG@CALB sample), we noted that the vibration bands at 1644 cm^{-1} (C=N bond) and 1553 cm^{-1} (N-H bending of free amines in protein) were further increased in intensity compared to the enzyme-free support, confirming successful anchoring of the biocatalyst (Figure 5 A,d).

From the thermogravimetric analysis (Figure 5 B), the amount of functional groups anchored on the silicified hydrogel was estimated by the difference between the mass loss of the functionalized matrix minus the mass loss of the bare Sihgel. In order to minimize the effects of solvent incorporated into the pores, the weight loss below $180\text{ }^{\circ}\text{C}$ was not taken into consideration. Covalent anchoring of CTMS (Sihgel@C) (Figure 5 B,a) and APTMS (Sihgel@A) (Figure S6, ESI) yielded a weight loss of 4.5 % and 6.6% due to the decomposition of trimethyl groups and aminopropyl groups respectively. Crosslinking with GAH (Sihgel@AG) (Figure 5 B,b) yielded a weight loss of 11.7 % resulting from the decomposition of glutaraldehyde-activated aminopropyl groups. Note that the weight loss measured on Sihgel@CAG was slightly higher (*ca.* 2.2%) compared to Sihgel@C and Sihgel@AG taken together indicating that APTMS and GAH have a positive effect in promoting the loading capacity of CTMS (Figure 5 B,c).

The grafting densities (D_g) of trimethyl and aminopropyl groups on Sihgel@C and Sihgel@A matrices were estimated to be 45 mg/g and 66 mg/g respectively. Using Equation 1 (see ESI), the corresponding surface coverages (S_{cov}) were determined to be 0.24 chain/nm² and 0.28 chain/nm² respectively. Assuming that APTMS was fully hydrolyzed and considering that organosilanes formed a monolayer, it was then possible to estimate the maximum densities of trimethyl and aminopropyl groups that could be grafted on the surface of the host matrix. Thus, considering that the occupied surface area of trimethyl groups is 0.43 nm^2 ,⁴⁸ and each aminopropyl ligand occupies a surface of 0.2 nm^2 ,⁴⁹ the maximum grafting densities (D_g^{max}) were determined to be 57 mg/g and 68 mg/g respectively (Equation 2, ESI). As the experimental results are in close agreement with

the theoretical predictions, this means that organosilanes most likely form a monolayer on the surface of the hybrid material.

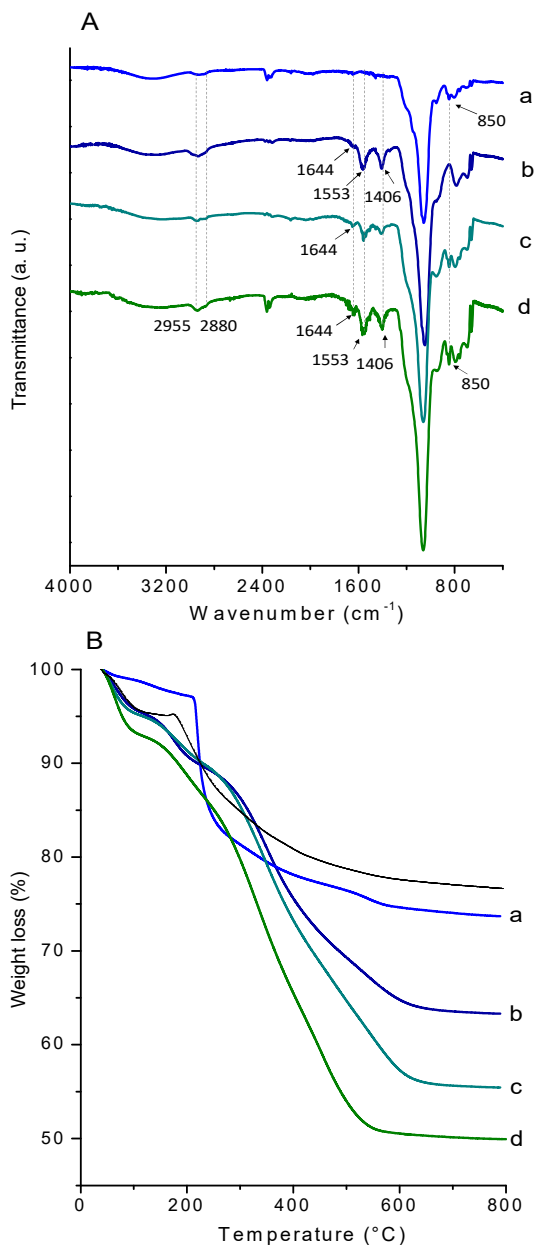


Figure 5. ATR-FTIR spectra (A) and TGA curves (B) of the silicified F127/ α -CD hydrogel modified with different functional groups: (a) Sihgel@C, (b) Sihgel@AG, (c) Sihgel@CAG and (d) Sihgel@CAG@CALB. The TG profile of non-functionalized Sihgel is added for comparison (dotted line).

Although the protein content cannot be determined exactly by TG analysis, an estimation can be provided from the difference in the mass loss between Sihgel@CAG@CALB (Figure 5 B,d) and Sihgel@CAG (Figure 5 B,c). Thus, we found that the effective weight loss corresponding to the decomposition of the enzyme was 5.7 % (Table S1, ESI). This value is much higher than that measured on the control Sisg@CAG@CALB catalyst prepared without hydrogel under identical conditions (1.1%) (Figure S7, ESI), therefore confirming the importance of the porous structure on the protein loading capacity.

N₂-adsorption analyses were then carried out to determine changes in the textural characteristics of the silicified hydrogel upon silanization and enzyme immobilization (Figure 6 a-d). Sihgel@CAG showed a decrease in both surface area (from 136 to 54 m²/g) and pore volume (from 0.156 to 0.139 cm³/g) with respect to Sihgel; however, no pore blocking effects were evidenced in these solids (Table S1, ESI). In fact, the pore size distributions of all functionalized supports were similar to that of the Sihgel matrix, supporting the hypothesis that organosilanes most likely form a thin layer, in agreement with thermogravimetric results. On the other hand, the broadening of the pore size distributions upon functionalization (Figure 6 a-c) indicates that some silanes could also be anchored on the surface of the support carrier.⁵⁰ The alteration of the pore architecture upon functionalization with APTMS and glutaraldehyde (Figure 6 b) may be due to the ability of this linker to yield cross-linking reactions in interaction with the amino groups grafted on the support surface.⁵¹ Importantly, in comparison with the enzyme-free Sihgel@CAG matrix, the supported biocatalyst (Figure 6 d, Table S1, ESI) presented a marked decrease in pore volume (0.094 cm³/g) and surface area (39 m²/g) which is typical of the filling of the pores with the protein.⁵² Considering the dimensions of CALB (3.0 nm x 4.0 nm x 5.0 nm),⁵³ this lipase is likely

to locate in the largest mesopores (20-60 nm) and macropores (1-3 μm) of the support, but not in the smallest mesopores (3-4 nm) and micropores (< 2 nm). Accordingly, protein immobilization implied narrowing of the second pore size distribution with respect to Sihgel@CAG (Figure 6 c) and reduction of the average pore diameter to 20-50 nm (Figure 6 d). Interestingly, despite the variations noted on the textural characteristics of the functionalized support, the hierarchical pore structure remained intact after lipase immobilization, which could be beneficial for the mass transfer within the pores during the catalytic reaction.

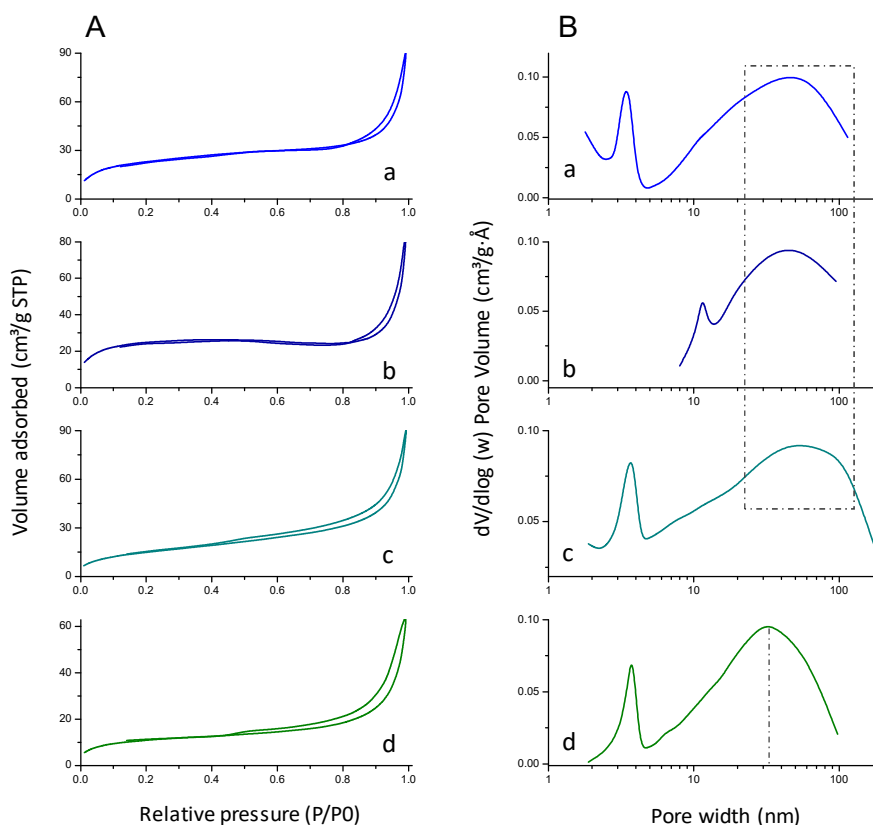


Figure 6. N₂-adsorption isotherms (A) and corresponding pore size distributions (B) of (a) Sihgel@C, (b) Sihgel@AG, (c) Sihgel@CAG and (d) Sihgel@CAG@CALB.

Incorporation of CALB on the silicified hydrogel was further confirmed by laser scanning confocal microscopy (CLSM) using fluorescein isothiocyanate (FITC) as the fluorescent dye.

FITC contains an isothiocyanate functional group ($-N=C=S$) which is reactive toward nucleophiles such as amine or thiol groups found in proteins.⁵⁴ The fluorescence micrograph of the Sihgel@CAG support loaded with FITC-labelled CALB appeared bright green and presented uniform intensity distribution indicating uniform dispersion of the lipase within the porous matrix (Figure 7 a-c). On the other hand, the Sihgel@CAG support loaded with FITC, but without lipase, displayed less fluorescence due to the lower amount of available $-NH_2$ groups originating only from the functionalized matrix (Figure 7 d). Indeed, as shown previously by Ara *et al.*,⁵⁵ the FITC dye has the ability to bind the amino-terminated silica surfaces through its isothiocyanate functional groups and a successful large-scale binding has been demonstrated by fluorescence measurements.⁵⁵

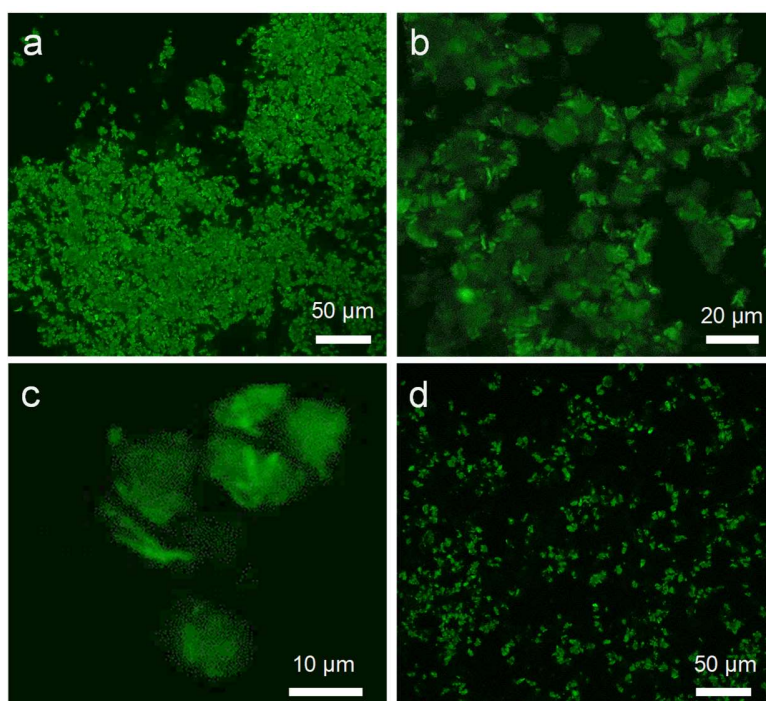


Figure 7. Laser scanning confocal micrograph of (a-c) FITC-labelled lipase CALB loaded on the Sihgel@CAG support at different magnifications and (d) lipase-free FITC loaded on the Sihgel@CAG support.

Catalytic activity

The catalytic activity of the immobilized lipase was then evaluated in the oxidation of DFF to FDCA. Reaction was assessed by adding aqueous hydrogen peroxide (30% v/v) to a mixture of ethyl acetate (EtOAc) and *tert*-butanol (tBuOH) (1:1 v/v).³⁹ The number of equivalents of H₂O₂ used was 2.0, which represents the optimum amount required to obtain maximum enzyme activity. Reaction products were analyzed by ¹H NMR spectroscopy (Figures S8-S10, ESI) and HPLC (Figures S11-S13, ESI). Results showing the effect of the immobilization method, the porosity of the matrix and the nature of functional groups are summarized in Table 1.

Initially, we investigated the activity of the enzyme immobilized by ionic binding and hydrophobic interactions on the support modified solely with hydrophobic groups (CTMS) as a function of the enzyme loading varying from 2 mg (1.33 mg/mL CALB) to 8 mg (5.33 mg/mL) in the immobilization solution. For the catalysts prepared with 2 mg CALB, the CTMS/SiO₂ molar ratio was varied between 0.15 and 0.50. In order to examine the effect of hydrogel incorporation, the material calcined at 500 °C and functionalized with a CTMS/SiO₂ molar ratios of 0.33 was also used as support for comparison. Under those conditions, both trimethylsilyl and silanol groups are available on the surface to interact with the enzyme, their proportion depending on the composition of the silane layer (amount of CTMS used) and the nature of the matrix (calcined or as-synthesized).

The isoelectric point (pI) of CALB was previously reported to be 6.0.³⁴ The pI is the point at which the total net charge on the enzyme is zero and it depends on the nature and distribution of surface functional groups such as -NH₂, -COOH, -OH.⁵⁶ When the pH of solution is below the pI, the net charge of the enzyme is positive and it is negative when the pH is above the pI. For the

immobilization of CALB, we chose a pH of 4.6 (acetate buffer) at which the enzyme is predominantly positively charged, while the silica support is negatively charged (the point of zero charge of silica was reported to be between pH 2.0 and pH 3.5).⁵⁷ On the other hand, the pH of the reaction medium was 4.8, close to the pH of the immobilization, which permits to maintain the enzyme fixed on the support during the catalytic reaction. Under those conditions, the immobilization efficiency determined using Bradford protein assay was 93-95% (Equation 3, ESI), while the loading capacity ranged between 9.5 and 37.2 wt. % (Equation 4, ESI) (Table 1).

As expected, the overall activity showed a strong dependence on enzyme loading. While the free lipase was not active under the experimental conditions employed (entry 1), the immobilization of 2 mg CALB on the hydrophobic silica (entry 2) resulted in 88% DFF conversion after 7 hours of reaction at 40 °C. However, the major product was FFCA (69%), with only minor yields of FDCA (19%). On the other hand, the increase of the lipase loading to 4 mg (2.67 mg/mL) and 8 mg (5.33 mg/mL) led to a complete conversion of DFF (entries 3 and 4), regardless the enzyme loading, and resulted in more than 4-fold increase in the FDCA yield (85%, entry 4). The maximum specific activity was obtained with 4 mg CALB ($18.3 \mu\text{mol g}^{-1} \text{min}^{-1}$) corresponding to a total turnover number (TTN) of approximately 254 and a turnover frequency (TOF) of 0.604 min^{-1} (entry 3).

It is well-known that the active site of lipases is naturally covered by a lid. It is assumed that the conformational changes that proteins undergo at hydrophobic/hydrophilic interfaces promote the opening of the lid, thus making the active site accessible to the substrate.⁵⁸ As suggested by several studies,^{59,60} proteins adsorb preferentially on hydrophobic surfaces through their hydrophobic moieties, while on hydrophilic surfaces, the strong water-surface interactions tend to shield the enzyme from the support causing its desorption. However, on hydrophobic surfaces, proteins undergo more conformational changes and display more denatured structures than they do on

hydrophilic surfaces. Consequently, an optimum hydrophilic/hydrophobic balance is necessary to counter the negative effects caused by the excess of hydrophobic groups.

CALB is an atypical lipase in the sense that it does not possess a lid, but presents interfacial hyperactivation though. Thus, upon contact with hydrophobic surfaces, this lipase is supposed to adopt a specific orientation by exposing its active site toward the substrate.⁶¹ We found that the optimum CTMS/SiO₂ molar ratio required to obtain maximum enzyme activity was 0.33 (entry 2). Higher or lower ratios caused a decrease in the enzymatic performance (entries 5, 6) confirming the critical role played by the hydrophobic groups in lipase activation.

Notably, the removal of the hydrogel from the silica support by calcination, prior to surface functionalization, resulted in a decrease of the FDCA yield from 73% (entry 3) to 55% (entry 7), although the specific surface area of this material was very high and the hierarchical pore structure was preserved (Figure S4 and Table S1, ESI). The specific activity, TTN and TOF followed the same decreasing trend as the FDCA yield, indicating that the pore architecture is not the only factor to affect the catalytic performance.

Table 1. Catalytic performance of immobilized lipase CALB in the oxidation of DFF to FDCA.^a

Entry	Catalyst	Immobilization efficiency (%) ^b	Loading capacity (wt.%) ^c	DFF conversion (%)	Yield (%)		Specific activity ($\mu\text{mol g}^{-1} \text{min}^{-1}$) ^k	TTN (mol mol^{-1}) ^l	TOF (min^{-1}) ^m
					FFCA (%)	FDCA (%)			
1	Free CALB	-	-	0	0	0	0	0	0
Ionic binding and hydrophobic interactions									
2	Sihgel@C ^d @CALB ^c	95	9.5	88	69	19	9.5	132.0	0.314
3	Sihgel@C@CALB-4mg	95	19.0	100	27	73	18.3	253.6	0.604
4	Sihgel@C@CALB-8mg	93	37.2	100	15	85	10.9	150.8	0.359
5	Sihgel@C0.15@CALB	70	7.0	0	0	0	0.0	0.0	0.000
6	Sihgel@C0.50@CALB	73	7.3	72	72	0	0.0	0.0	0.000
7	Sihgel-T500 ^f @C@CALB-4mg	89	17.8	100	45	55	14.7	203.9	0.486
Grafting									
8	Sihgel@AG@CALB	89	8.9	44	44	0	0.0	0.0	0.000
9	Sihgel@CAG@CALB	96	9.6	100	33	67	33.2	460.6	1.097
10	Sihgel@CAG@CALB-24h ^g	96	9.6	100	<1	>99	>14.3	>680.0	>0.473
11	Sihgel@C0.25AG@CALB	91	9.1	87	62	25	13.1	181.3	0.432
12	Sihgel@C0.38AG@CALB	94	9.4	94	69	25	12.7	175.5	0.418
13	Sihgel@C0.43AG@CALB	94	9.4	78	63	15	7.6	105.3	0.251
14	Sisg ^h @CAG@CALB	72	7.2	24	24	0	0.0	0.0	0.000
15	Sihgel-T500@CAG@CALB	88	8.8	85	68	17	9.2	127.5	0.304
16	SiF127 ⁱ @CAG@CALB	90	9.0	77	68	9	4.8	66.0	0.157
17	Si α -CD ^j @CAG@CALB	86	8.6	74	58	16	8.9	122.8	0.292

^aReaction conditions: 10 mM DFF, 2 mL EtOAc/tBuOH (1:1, v/v), sequential addition of 2.0 equivalents aqueous H₂O₂ (30% v/v) every hour for seven hours, temperature 40 °C, reaction time 7 hours, ^bCalculated from Equation 3 (see ESI), ^cCalculated from Equation 4 (see ESI), ^dCTMS/SiO₂ molar ratio = 0.33, ^e2 mg CALB in 20 mg support (1.33 mg/mL CALB in the immobilization solution), ^fthe silicified hydrogel was calcined at 500 °C before surface functionalization and enzyme immobilization, ^greaction time = 24 hours, ^htemplate-free sol-gel silica, ⁱF127-templated SiO₂, ^j α -CD-templated SiO₂, ^kspecific activity was calculated as μmol of product formed (two μmol peracid per μmol of FDCA) per g of protein in one minute, ^lTTN = moles of FDCA formed divided by moles of protein, ^mTOF = TTN divided by reaction time.

On the other hand, when the enzyme was grafted on the Sihgel@AG support silanized only with amino groups and activated with glutaraldehyde, the conversion of DFF dramatically dropped to 44%, while no FDCA was formed (entry 8). This confirms that the hydrophobic trimethyl groups of CTMS are crucial for the interfacial activation of the lipase. Moreover, the local hydrophobic microenvironment created by the CD-based nanocrystallites within the hydrogel is also likely to contribute to this mechanism by modulating the biocatalyst interactions at the interface.²⁶

Interestingly, the catalytic performance was further improved by anchoring 2 mg CALB on the Sihgel@CAG support silanized with both grafting and hydrophobic functions (entry 9). The increase of the immobilization efficiency with respect to Sihgel@AG (96% vs. 89%, Table 1) is likely due to hydrophobic enzyme-support interactions that occur in addition to covalent bond.^{40,62} Note that the FDCA yield of Sihgel@CAG@CALB has increased by 48% compared to the Sihgel@C@CALB catalyst prepared by ionic binding (entry 2), although the loading capacities were very close (9.6 wt.% vs. 9.5 wt.%). Similarly, the specific activity, TTN and TOF of the grafted enzyme were more than three times higher than those obtained with the adsorbed one. In addition, kinetics of Sihgel@CAG@CALB were much faster with respect to Si@C@CALB (Figure S14, ESI) indicating higher stability of the grafted enzyme.⁶² However, the reactions were slow to start up due to the diffusion barrier created by the substrate in interaction with the hydrogel surface (Figure S 14, ESI).

Notably, total DFF conversion with quantitative yield in FDCA (>99%) was achieved by increasing the reaction time to 24 h, accumulating a TTN higher than 680 (entry 10). Our results can be compared with those reported by Qin *et al.*³⁹ who obtained 88% yield in FDCA after 24 h at 40°C using commercially available immobilized CALB (Novozym 435). The amount of CALB employed by the authors was 9.6 mg for 22.5 mM DFF, corresponding to a TTN of 293; however,

the reaction conditions were not optimized. In line with the results obtained by ionic binding, we noted that small variations in the CTMS/SiO₂ molar ratio induced strong alteration of the overall lipase activity (entries 11-13). At low CTMS/SiO₂ molar ratios, the surface of the carrier was not sufficiently hydrophobic to enable interfacial activation of the lipase, while at high CTMS/SiO₂ molar ratios, the functional behavior of the protein was altered due to partial unfolding and spreading on the hydrophobic surface.^{59,60} Another relevant observation is that the porosity of the silicified hydrogel has also a strong impact on the catalytic performance. Thus, using conventional sol-gel silica prepared without template as a carrier resulted in a drastic drop of the immobilization efficiency to 72%; the DFF conversion also dropped to 24%, while no FDCA was formed (entry 14). Similarly, grafting of the lipase on the hierarchical pore structure of the calcined silica material gave 17% yield in FDCA, although the DFF conversion was relatively high (85%) (entry 15). Moreover, using pluronic F127 (entry 16) and α -CD (entry 17) separately as templates resulted in a severe decrease of the FDCA yield to 9% and 16% respectively with simultaneous reduction of the specific activity, TTN and TOF.

The overall picture emerging from our experimental results is that, in addition to surface chemistry, there are three other potential factors that contribute to the biocatalyst activity. These factors include (i) the pore architecture of the silica framework, (ii) the fibrous network created by the *polypseudorotaxanes* and (iii) the flexible surface of the incorporated hydrogel.

(i) As the substrate molecules diffuse to the entire volume of the carrier and not only on its surface, the multidimensional and interconnected pore structure of the silicified hydrogel offers possibility to improve mass transfer, thus permitting acceleration of the reaction kinetics. Indeed, our results confirm that the multiscale pore network of the silicified hydrogel has the ability to accommodate high enzyme loadings implying improvement of the overall activity with respect to

the template-free sol-gel silica (Sisg) and monomodal Si α CD and SiF127 materials. The unique arrangement of polypseudorotaxanes in a multimodal interconnected pore network provides a balance between small mesopores with large surface area for enhanced surface coverage, large mesopores with optimal size for the enzyme confinement and interconnected macropores for improved accessibility of the substrate to the active sites of the biocatalyst during the catalytic reaction.

(ii) The surface nanotopography is another important factor that can affect protein functionality. For instance, Jandt *et al.*^{60,63-65} established on the basis of atomic force microscopy that well-aligned nanocrystalline lamella interconnected by amorphous interlayers could trigger preferential lateral orientation of fibrinogen proteins along specific crystallographic directions and guide their assembly into network structures.⁶⁵ Interestingly, such preferential orientation was induced by topographical nanopatterns one order of magnitude smaller than the dimensions of the protein.⁶⁴

In contrast with conventional sol-gel silica, which tends to form random-shaped particles, the silicified hydrogel presents a fibrous-like structure originating from the self-assembly of elongated PEO/ α -CD polypseudorotaxanes into tightly packed nanocrystallites (Figure 4). In this sense, those nanocrystallites, which are present throughout the hydrogel, may also trigger more energetically favorable protein structures, thus permitting modulation of biocatalyst activity.⁶⁰

(iii) Finally, the soft nature of the incorporated hydrogel is another critical parameter that can influence the flexibility level of proteins within the pores.⁶⁰ We thus noted that the removal of the hydrogel from silica by calcination, prior to surface functionalization, resulted in almost 4-fold decrease in the FDCA yield and specific activity (entry 15 *vs.* entry 9), although the hierarchical pore structure of this material was preserved (Figure S4, d). Similar evidence was found with the non-calcined hydrogel-free silica where the DFF conversion dropped to 24% while no FDCA was

formed (entry 14). The likely reason for this behavior is that on the rigid surface of the solid carrier, the unfolding-refolding motion of the protein could be restricted, thus creating an energy barrier to the lid movement. In contrast, the smooth and confined space of the hydrogel can reduce protein-protein interactions and increase protein flexibility within the pores.

To understand if there is any possible interaction between the lipase CALB and α -CD incorporated within the pores, we performed DLS measurements on an enzymatic solution (2 mg/mL CALB) prepared with increasing concentrations of α -CD (from 0 to 23 mg/mL). The hydrodynamic radius of CALB aggregates, initially centered at 5.5 and 21 nm, increased continuously with α -CD addition reaching 11 and 42 nm at 23 mg/mL α -CD (Figure S15, ESI). Similarly, the addition of a small amount of CALB (1 mg/mL) to a concentrated α -CD solution (47 mg/mL) provoked the dissociation of the cage-type α -CD aggregates, confirming interaction between the two entities (Figure S16, ESI). Such interactions have been proven to be effective in enhancing by several orders of magnitude the activity and enantioselectivity of enzymes in organic solvents.⁶⁶ Barletta *et al.*⁶⁶ ascribed this observation to the ability of cyclodextrins to regulate the functional behavior of the enzyme by decreasing its rigidity and providing a favorable flexibility.

In the light of these findings, we were then interested in evaluating the recyclability and reusability of the supported lipase. We tried to use the Sihgel@CAG@CALB biocatalyst without any modification, but the enzyme was totally deactivated after the first run. As reported by Karich *et al.*,⁶⁷ the conversion of FFCA to FDCA catalyzed by peroxygenase from *Agrocybe aegerita* (AaeUPO) in the presence of H₂O₂ exhibits a pH-dependent behavior. While most of the FDCA was produced below pH 6.0, a complete deactivation of the enzyme was observed between pH 2.0 and 4.0. Considering that our reaction was performed at pH 4.8, FFCA and FDCA formed during the oxidation of DFF could trigger further pH decrease by diffusing into the pores where the protein

is confined. As both of these products bear carboxylic acid functions in their furanic cycle, the pH gradient created by their adsorption on the biocatalyst surface may therefore be responsible for the inhibition of the enzyme activity. We thus noticed a decrease in the pH of reaction mixture to 3.1 after the first run. Such a pH decrease may also cause some leakage of the lipase immobilized by ionic binding due to the beginning of protonation of silanol groups (SiOH_2^+) (the point of zero charge of silica is between pH 2.0 and pH 3.5). Moreover, for the grafted catalysts, the decrease in pH may also cause hydrolysis of the imine bond, implying leakage of the lipase.

To overcome this problem, polymers are commonly used as stabilizers as they protect enzymes from denaturing conditions by decreasing the pH gradient created on their surface.⁶⁸ We therefore opted for covering our biocatalyst with a pH-sensitive polymer, the poly(4-vinylpyridine) (P4VP). P4VP has a pKa value of approximately 4.5 and is able to swell upon protonation.⁶⁹ Under the immobilization conditions employed (acetate buffer, pH 4.6), P4VP is near neutral, therefore no electrostatic interactions may occur between the polymer and the enzyme. However, because of the presence of pyridine units on its structure, P4VP can readily serve as a hydrogen bond donor or acceptor.⁷⁰ In consequence, favorable hydrogen bond interactions may occur between the pyridine units of P4VP and the surface functional groups of the enzyme leading to spontaneous self-assembly.

Under those modified conditions, we evaluated the recycling use of the Sihgel@CAG@CALB biocatalyst prepared with 2 mg CALB and 20 wt.% P4VP after 24 hours of reaction time at 40 °C. The immobilized lipase was collected through centrifugation after each reaction cycle, rinsed with the EtOAc/tBuOH (1:1, v/v) mixture and subsequently dried under vacuum before being reutilized. As shown in Figure 8, full conversion of DFF could be achieved after five consecutive catalytic runs indicating that the confined lipase could withstand the reaction conditions. Importantly, the

FDCA yield was quantitative (>99%) after the initial two runs. Then, after the third run, it decreased to 72%, FFCA being the only intermediate. Some leakage of the lipase from the bioreactor can certainly occur, however a large part this decrease can mainly be attributed to the cumulative particle losses along filtration that caused reduction in the percentage amount of the biocatalyst remaining in the reaction mixture. In fact, complete recovery of the solid was not possible because of the presence of a large number of small-size particles in the silica matrix that remained dispersed in the reaction medium or were lost through successive rinsing steps. Actually, the amount of recovered catalyst after the fifth run (7.5 mg) represented almost one-third of the amount used during the first run (21.0 mg).

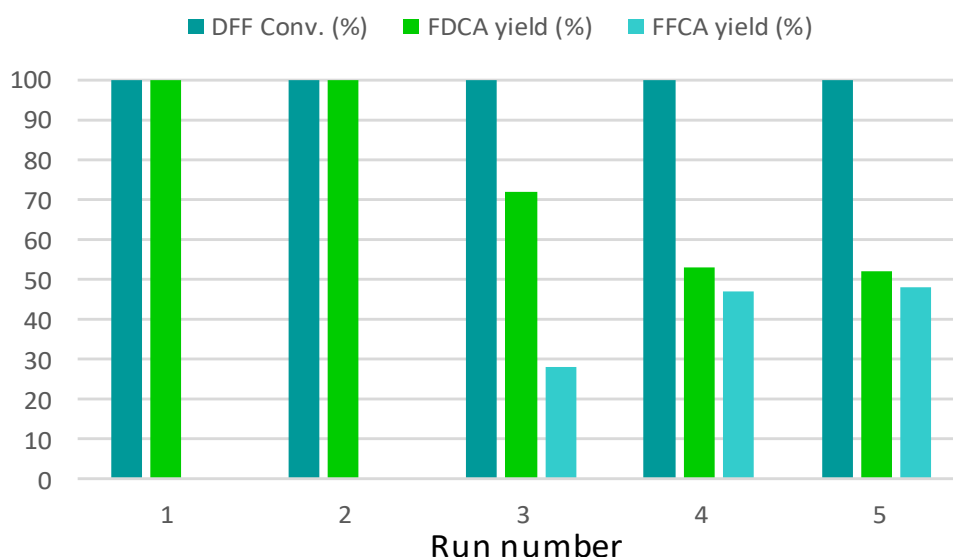


Figure 8. Catalytic recyclability of Sihgel@CAG@CALB biocatalyst. Reaction conditions: 10 mM DFF, 2 mL EtOAc/tBuOH (1:1, v/v), 2.0 equivalents aqueous H₂O₂ (30% v/v) at the beginning of the test, then after every hour for six hours, temperature 40 °C, reaction time 24 hours.

Importantly, we noticed that the rinsing solution was able to efficiently catalyze the oxidation of DFF (100% conversion) (Figure S17, ESI). As free lipase was not active in this reaction, it is

conceivable that this activity results from the enzyme anchored on small particles that were lost with rinsing. Indeed, once the small particles were removed, the FDCA yield remained constant (more than 50 %) in the following two cycles.

Conclusions

In this study, we have developed a straightforward approach for the confinement of lipase CALB within a hierarchically porous hybrid material. The supramolecular hydrogel network formed by host-guest interactions between the block copolymer pluronic F127 and the native α -cyclodextrin (α -CD) was first silicified by sol-gel reaction using tetramethylorthosilicate (TMOS) as silica source. After modification with hydrophobic and chemically reactive groups, this material was used as matrix for the confinement of lipase CALB. The cross-linked hydrogel network showed high loading efficiency and allowed to increase the softness and flexibility of silica permitting modulation of the enzymatic activity in the selective oxidation of DFF to FDCA. Three potential factors were identified to contribute to the catalytic performance of the lipase: (i) the hierarchically interconnected pore structure of the support carrier, (ii) the fibrous topography of the nanocrystallites and (iii) the soft nature of the supramolecular hydrogel. These three factors were found to concomitantly affect the mass transfer rate of reactants and products as well as the conformational flexibility of protein on the surface of the carrier. A very delicate balance between them was essential for preserving the three-dimensional structure of the active site and regulating the functional behavior of the biocatalyst. The confinement of enzymes within supramolecular architectures opens new avenues for future development of enzymatic nanoreactors with a range of promising properties for biocatalytic and biotechnological applications.

ASSOCIATED CONTENT

Supporting Information

Experimental details, DLS measurements and visual aspect of F127/ α -CD solutions, DLS of CALB/ α -CD mixtures, N₂ adsorption isotherms, FE-SEM images, TG and FTIR curves, ¹H NMR spectra and HPLC chromatograms of isolated products and reaction mixtures.

Conflicts of interest

The authors declare no competing financial interests.

Corresponding Author:

*E-mail: rudina.bleta@univ-artois.fr

ACKNOWLEDGMENT

C. Decarpigny is grateful to the Région Hauts-de-France and the University of Artois for the PhD grant. Chevreul Institute (FR 2638), Ministère de l'Enseignement Supérieur, de la Recherche et de l'Innovation and FEDER are acknowledged for supporting and funding this work. We thank Dr E. Richard for access to CLSM and technical advices, as well as the Research Federation FRABio (Univ. Lille, CNRS, FR 3688) for providing the scientific and technical environment conducive to achieving this work. We are grateful to Mr D. Prevost, Dr A. Addad and Dr J. Ternel for technical assistance with the reactor setup, Electron Microscopy and NMR respectively, as well

as Dr N. Kania for help with HPLC and TG analyses. The TEM facility in Lille is supported by the Conseil Regional des Hauts-de-France and the European Regional Development Fund (ERDF).

REFERENCES

[1] Shoda, S.; Uyama, H.; Kadokawa, J.; Kimura, S.; Kobayashi, S., Enzymes as green catalysts for precision macromolecular synthesis. *Chem. Rev.* **2016**, *116*, 2307-2413.

[2] Bommarius, A. S.; Paye, M. F., Stabilizing biocatalysts. *Chem. Soc. Rev.* **2013**, *42*, 6534-6565.

[3] Chapman, J.; Ismail, A. E.; Dinu, C. Z., Industrial applications of enzymes: Recent advances, techniques, and outlooks. *Catalysts* **2018**, *8*, 238.

[4] Roy, I.; Prasad, S., Converting enzymes into tools of industrial importance. *Recent Pat. Biotechnol.* **2017**, *12*, 33-56.

[5] Franssen, M. C. R.; Steunenberg, P.; Scott, E. L.; Zuilhof, H.; Sanders, J. P. M., Immobilised enzymes in biorenewables production. *Chem. Soc. Rev.* **2013**, *42*, 6491-6533.

[6] Sheldon, R. A.; van Pelt, S., Enzyme immobilisation in biocatalysis: why, what and how. *Chem. Soc. Rev.* **2013**, *42*, 6223-6235.

[7] Mann, S., Life as a nanoscale phenomenon. *Angew Chem Int Ed Engl.* **2008**, *47*, 5306-5320.

[8] Kerfeld, C. A.; Sawaya, M. R.; Yeates, T. O., Protein structures forming the shell of primitive bacterial organelles. *Science* **2005**, *309*, 936-938.

-
- [9] Luckarift, H. R.; Spain, J. C.; Naik, R. R.; Stone, M. O., Enzyme immobilization in a biomimetic silica support. *Nature Biotechnology* **2004**, *22*, 211-213.
- [10] Kuchler, A.; Yoshimoto, M.; Luginbühl, S.; Mavelli, F.; Walde, P., Enzymatic reactions in confined environments. *Nature Technology* **2016**, *11*, 409-420.
- [11] Ariga, K.; Ji, Q.; Mori, T.; Naito, M.; Yamauchi, Y.; Abe, H.; Hill, J. P., Enzyme nanoarchitectonics: organization and device application. *Chem. Soc. Rev.* **2013**, *42*, 6322-6345.
- [12] Gao, J.; Kong, W.; Zhou, L.; He, Y.; Ma, L.; Wang, Y.; Yin, L.; Jiang, Y., Monodisperse core-shell magnetic organosilica nanoflowers with radial wrinkle for lipase immobilization. *Chem. Eng. J.* **2017**, *309*, 70-79.
- [13] Liang, K.; Ricco, R.; Doherty, C.M.; Styles, M.J.; Bell, S.; Kirby, N.; Mudie, S.; Haylock, D.; Hill, A.J.; Doonan, C.J.; Falcaro, P., Biomimetic mineralization of metal-organic frameworks as protective coatings for biomacromolecules. *Nat. Commun.* **2015**, *6*, 7240-7247.
- [14] Du, Y.; Gao, J.; Zhou, L.; Ma, L., He, Y.; Huang, Z.; Jiang, Y., Enzyme nanocapsules armored by metal-organic frameworks: A novel approach for preparing nanobiocatalyst. *Chem. Eng. J.* **2017**, *327*, 119-1197.
- [15] Kim, J.; Grate, J. W., Single-enzyme nanoparticles armored by a nanometer-scale organic/inorganic network. *Nano Lett.* **2003**, *3*, 1219-1222.
- [16] Lei, C.; Shin, Y.; Liu, J.; Ackerman, E. J., Synergetic effects of nanoporous support and urea on enzyme activity. *Nano Lett.* **2007**, *7*, 1050-1053.
- [17] Huo, J.; Aguilera-Sigalat, J.; El-Hankari, S.; Bradshaw, D., Magnetic MOF microreactors for recyclable size selective biocatalysis. *Chem. Sci.* **2015**, *6*, 1938-1943.

[18] Du, Y.; Gao, J.; Zhou, L.; Ma, L., He, Y.; Zheng, X.; Huang, Z.; Jiang, Y., MOF-based nanotubes to hollow nanospheres through protein-induced soft-templating pathways, *Adv. Sci.* **2019**, *6*, 1801684.

[19] Kishida, A.; Ikada, Y. in *Polymeric Biomaterials*, S. Dumitriu ed. (Marcel Dekker, USA, **2002**).

[20] Drury, J. L.; Mooney, D. J., Hydrogels for tissue engineering: scaffold design variables and applications. *Biomaterials* **2003**, *24*, 4337-4351.

[21] Vermonden, T.; Censi, R.; Hennink, W. E., Hydrogels for protein delivery. *Chem. Rev.* **2012**, *112*, 2853-2888.

[22] Schnepf, Z.; Gonzalez-McQuire, R.; Mann, S., Hybrid biocomposites based on calcium phosphate mineralization of self-assembled supramolecular hydrogels. *Adv. Mater.* **2006**, *18*, 1869-1872.

[23] Yang, Z. M.; Xu, B., A simple visual assay based on small molecule hydrogels for detecting inhibitors of enzymes. *Chem. Commun.* **2004**, 2424-2425.

[24] Wang, Q.; Yang, Z.; Zhang, X.; Xiao, X.; Chang, C. K., Xu, B., A supramolecular-hydrogel-encapsulated hemin as an artificial enzyme to mimic peroxidase. *Angew. Chem.* **2007**, *119*, 4363-4367.

[25] Wang, Q.; Yang, Z.; Wang, L.; Ma, M.; Xu, B., Molecular hydrogel-immobilized enzymes exhibit superactivity and high stability in organic solvents. *Chem. Commun.* **2007**, 1032-1034.

[26] Liu, K. L.; Zhang, Z. X.; Li, J., Supramolecular hydrogels based on cyclodextrin-polymer polypseudorotaxanes: materials design and hydrogel properties. *Soft Matter* **2011**, *7*, 11290-11297.

[27] Harada, A.; Kamachi, M., Complex formation between cyclodextrin and poly (propylene glycol). *J. Chem. Soc. Chem. Commun.* **1990**, *19*, 1322-1323.

[28] Breslow, R., Biomimetic chemistry and artificial enzymes: Catalysis by design. *Acc. Chem. Res.* **1995**, *28*, 146-153.

[29] Travelet, C.; Schlatter, G.; Hebraud, P.; Brochon, C.; Lapp, A.; Anokhin, D. V.; Ivanov, D. A.; Gaillard, C.; Hadziioannou, G.; Multiblock copolymer behaviour of α -CD/PEO-based polyrotaxanes: towards nano-cylinder self-organization of α -CDs. *Soft Matter* **2008**, *4*, 1855-1860.

[30] Travelet, C.; Schlatter, G.; Hebraud, P.; Brochon, C.; Lapp, A.; Hadziioannou, G., Formation and self-organization kinetics of α -CD/PEO-based pseudo-polyrotaxanes in water. A specific behavior at 30 °C. *Langmuir* **2009**, *25*, 8723-8734.

[31] Travelet, C.; Hebraud, P.; Perry, C.; Brochon, C.; Hadziioannou, G.; Lapp, A.; Schlatter, G., Temperature-dependent structure of α -CD/PEO-based polyrotaxanes in concentrated solution in DMSO: kinetics and multiblock copolymer behavior. *Macromolecules* **2010**, *43*, 1915-1921.

[32] Houde, A.; Kademi, A.; Leblanc, D., Lipases and their industrial applications: an overview. *Appl Biochem Biotechnol.* **2004**, *118*, 155-170.

[33] Gao, J.; Wang, Y., Du, Y.; Zhou, L.; He, Y.; Ma, L.; Yin, L., Kong, W., Jiang, Y., Construction of biocatalytic colloidosome using lipase-containing dendritic mesoporous silica nanospheres for enhanced enzyme catalysis. *Chem. Eng. J.* 2017, *317*, 175-186.

[34] Kirk, O.; Christensen, M. W., Lipases from *Candida antarctica*: Unique biocatalysts from a unique origin. *Org. Process Res. Dev.* **2002**, *6*, 446-451.

[35] Anderson, E. M.; Larsson, K. M.; Kirk, O., One biocatalyst-many applications: the use of *Candida antarctica* B-lipase in organic synthesis. *Biocatal. Biotransform.* **1998**, *16*, 181-204.

[36] Sheldon, R. A., Green and sustainable manufacture of chemicals from biomass: state of the art. *Green Chem.* **2014**, *16*, 950-963.

[37] Krystof, M.; Perez-Sanchez, M.; Dominguez de Maria, P., Lipase-mediated selective oxidation of furfural and 5-hydroxymethylfurfural. *Chem. Sus. Chem.* **2013**, *6*, 826-830.

[38] Dijkman, W. P., Groothuis, D. E.; Fraaije, M. W., Enzyme-catalyzed oxidation of 5-hydroxymethylfurfural to furan-2,5-dicarboxylic acid. *Angew. Chem. Int. Ed.* **2014**, *53*, 6515-6518.

[39] Qin, Y. Z.; Li, Y. M.; Zong, M. H.; Wu, H.; Li, N., Enzyme-catalyzed selective oxidation of 5-hydroxymethylfurfural (HMF) and separation of HMF and 2,5-diformylfuran using deep eutectic solvents. *Green Chem.* **2015**, *17*, 3718-3722.

[40] Barbosa, O.; Torres, R. ; Ortiz, C. ; Berenguer-Murcia, Á. ; Rodrigues, R. C.; Fernandez-Lafuente, R., Heterofunctional supports in enzyme immobilization: From traditional immobilization protocols to opportunities in tuning enzyme properties. *Biomacromolecules* **2013**, *14*, 2433-2462.

[41] Alexandridis, P.; Holzwarth, J. F.; Hatton, T. A., Micellization of poly (ethylene oxide)-poly (propylene oxide)-poly (ethylene oxide) triblock copolymers in aqueous solutions: thermodynamics of copolymer association. *Macromolecules* **1994**, *27*, 2414-2425.

[42] Bleta, R.; Machut, C.; Leger, B.; Monflier, E.; Ponchel, A., Coassembly of block copolymer and randomly methylated β -cyclodextrin: From swollen micelles to mesoporous alumina with tunable pore size. *Macromolecules* **2013**, *46*, 5672-5683.

[43] Simoes, S. M. N.; Veiga, F.; Torres-Labandeira, J. J.; Ribeiro, A. C. F.; Sandez-Macho, M. I.; Concheiro, A.; Alvarez-Lorenzo, C., Syringeable Pluronic- α -cyclodextrin supramolecular gels for sustained delivery of vancomycin. *Eur. J. Pharm. Biopharm.* **2012**, *80*, 103-112.

[44] Bleta, R.; Manuel, S.; Léger, B.; Da Costa, A.; Monflier, E.; Ponchel, A., Evidence for the existence of crosslinked crystalline domains within cyclodextrin-based supramolecular hydrogels through sol-gel replication. *RSC Adv.* **2014**, *4*, 8200-8208.

[45] Vansant, E. F.; Van Der Voort, P.; Vrancken, K. C., Characterization and chemical modification of the silica surface. Elsevier, The Netherlands. **1995**.

[46] Grube, M.; Bekers, M.; Upite, D.; Kaminska, E., Infrared spectra of some fructans. *Spectroscopy* **2002**, *16*, 289-296.

[47] Impéror-Clerc, M.; Davidson, P.; Davidson, A., Existence of a microporous corona around the mesopores of silica-based SBA-15 materials templated by triblock copolymers. *J. Am. Chem. Soc.* **2000**, *122*, 11925-11933.

[48] Zhao, X. S.; Lu, G. Q., Modification of MCM-41 by surface silylation with trimethylchlorosilane and adsorption study. *J. Phys. Chem. B* **1998**, *102*, 1556-1561.

[49] Liu, Y.; Li, Y.; Li, X. M.; He, T., Kinetics of (3-aminopropyl) triethoxysilane (APTES) silanization of superparamagnetic iron oxide nanoparticles. *Langmuir* **2013**, *29*, 15275-15282.

[50] Reber, M. J.; Brühwiler, D., Mesoporous hybrid materials by simultaneous pseudomorphic transformation and functionalization of silica microspheres. *Part. Part. Syst. Char.* **2015**, *32*, 243-250.

[51] Chandran, P. L.; Paik, D. C.; Holmes, J. W., Structural mechanism for alteration of collagen gel mechanics by glutaraldehyde crosslinking. *Connect Tissue Res.* **2012**, *53*, 285-297.

[52] Giri, S.; Trewyn, B. G.; Stellmaker, M. P.; Lin, V. S. Y., Stimuli-responsive controlled-release delivery system based on mesoporous silica nanorods capped with magnetic nanoparticles. *Angew. Chem. Int. Ed.* **2005**, *44*, 5038-5044.

[53] Uppenberg, J., Ohmer, N.; Norin, M.; Hult, K.; Kleywegt, G. J.; Patkar, S.; Waagen, V.; Anthomen, T.; Jones, T.A., Crystallographic and molecular-modeling studies of lipase B from *Candida antarctica* reveal a stereospecificity pocket for secondary alcohols. *Biochemistry* **1995**, *34*, 16838-16851.

[54] Baumgärtel, T.; von Borczyskowski, C.; Graaf, H., Selective surface modification of lithographic silicon oxide nanostructures by organofunctional silanes. *Beilstein J. Nanotechnol.* **2013**, *4*, 218-226

[55] Ara, M.; Tsuji, M.; Tada, H., Preparation of amino-terminated monolayers via hydrolysis of phthalimide anchored to Si (1 1 1). *Surf. Sci.* **2007**, *601*, 5098-5102.

[56] Hanefeld, U.; Gardossi, L.; Magner, E., Understanding enzyme immobilization. *Chem. Soc. Rev.* **2008**, *38*, 453-468.

[57] Parks, G. A., The isoelectric points of solid oxides, solid hydroxides, and aqueous hydroxo complex systems. *Chem. Rev.* **1965**, *65*, 177-198.

-
- [58] Reis, P.; Holmberg, K.; Watzke, H.; Leser, M.; Miller, R., Lipases at interfaces: a review. *Adv. Colloid Interface Sci.* **2009**, *147*, 237-250.
- [59] Ouberai, M. M.; Xu, K.; Welland, M. E., Effect of the interplay between protein and surface on the properties of adsorbed protein layers. *Biomaterials* **2014**, *35*, 6157-6163.
- [60] Firkowska-Boden, I.; Zhang, X.; Jandt, K. D., Controlling protein adsorption through nanostructured polymeric surfaces. *Adv. Healthcare Mater.* **2018**, *7*, 1-19.
- [61] Zisis, T.; Freddolino, P. L.; Turunen, P.; van Teeseling, M. C. F.; Rowan, A. E.; Blank, K. G., Interfacial activation of *Candida antarctica* lipase B: Combined evidence from experiment and simulation. *Biochemistry* **2015**, *54*, 38, 5969-5979.
- [62] Rodrigues, R. C.; Berenguer-Murcia, A.; Fernandez-Lafuente, R.; Coupling chemical modification and immobilization to improve the catalytic performance of enzymes. *Adv. Synth. Catal.* **2011**, *353*, 2216-2238.
- [63] Keller, T. F.; Müller, M.; Ouyang, W.; Zhang, J. T.; Jandt, K. D., Templating α -helical poly(l-lysine)/polyanion complexes by nanostructured uniaxially oriented ultrathin polyethylene films. *Langmuir* **2010**, *26*, 18893-18901.
- [64] Helbing, C.; Stoessel, R.; Hering, D. A.; Arras, M. M. L.; Bossert, J.; Jandt, K. D., pH-dependent ordered fibrinogen adsorption on polyethylene single crystals. *Langmuir* **2016**, *32*, 11868-11877.
- [65] Keller, T. F.; Schönfelder, J.; Reichert, J.; Tuccitto, N.; Licciardello, A.; Messina, G. M. L.; Marletta, G.; Jandt, K. D., How the surface nanostructure of polyethylene affects protein assembly and orientation. *ACS Nano* **2011**, *5*, 3120-3131.

[66] Griebenow, K.; Laureano, Y. D.; Santos, A. M.; Clemente, I. M.; Rodriguez, L.; Vidal, M. W.; Barletta, G., Improved enzyme activity and enantioselectivity in organic solvents by methyl- β -cyclodextrin. *J. Am. Chem. Soc.* **1999**, *121*, 8157-8163.

[67] Karich, A.; Kleeberg, S. B.; Ullrich, R.; Hofrichter, M., Enzymatic preparation of 2,5-furandicarboxylic acid (FDCA)-A substitute of terephthalic acid by the joined action of three fungal enzymes. *Microorganisms* **2018**, *6*, 5.

[68] Virgen-Ortiz, J. J.; dos Santos, J. C. S.; Berenguer-Murcia, A.; Barbosa, O.; Rodrigues, R. C.; Fernandez-Lafuente, R., Polyethylenimine: a very useful ionic polymer in the design of immobilized enzyme biocatalysts. *J. Mater. Chem. B* **2017**, *5*, 7461-7490.

[69] Wang, H.; Lee, I. H.; Yan, M., A general method to determine ionization constants of responsive polymer thin films. *J. Colloid Interface Sci.* **2012**, *365*, 178-183.

[70] Nie, L.; Liu, S.; Shen, W.; Chen, D.; Jiang, M., One-pot synthesis of amphiphilic polymeric Janus particles and their self-assembly into supermicelles with a narrow size distribution. *Angew. Chem., Int. Ed.* **2007**, *119*, 6437-6440.

Table of Contents Graphic

